Optics Letters

Multi-stack InP/GaAsP quantum dot lasers on Si with high characteristic temperature

WEN GU, BOQUN ZHAO, XIANGQUAN LIU, AND KEI MAY LAU*

Division of Emerging Interdisciplinary Area, Hong Kong University of Science and Technology, Clear Water Bay, Kowloon, Hong Kong SAR, China
*eekmlau@ust.hk

Received 6 May 2026; revised 7 June 2026; accepted 11 June 2026; posted 15 June 2026; published 24 June 2026

Monolithic integration of InP quantum dot (QD) lasers on silicon is essential for on-chip quantum technologies and biophotonics. We demonstrate 780-nm InP/GaAsP QD lasers monolithically grown on (001) Si with an improved characteristic temperature (T_0) of 125 K in the 20–50 °C range. By increasing the active-region stacking to five layers, the threshold current density was reduced to 0.86 kA/cm^2 with a thermal wavelength shift of 0.25 nm/°C. Comparative analysis with 3-layer counterparts on Si and devices on GaAs substrates indicates that the optimized 5-layer structure effectively enhances modal gain and consequently the thermal stability of Si-based near-infrared light sources. This work suggests that active-layer stacking is a feasible strategy for improving the thermal characteristics of InP QD lasers on Si.

https://doi.org/10.1364/OL.604816

Monolithic integration of III–V semiconductor lasers on silicon (Si) is essential for scalable, low-cost, and high-density Si-based optoelectronics [1,2]. While research has matured at telecommunication wavelengths (1.3 and 1.5 µm), there is an increasing demand for light sources in the 700–800 nm near-infrared (NIR) range. This spectral window is of great importance for emerging applications, such as chip-scale quantum technologies [3], biophotonics [4], and spectroscopy [5]. However, achieving reliable NIR emission on Si remains a challenge, as direct epitaxial growth of III-V materials on Si is fundamentally hindered by lattice and thermal expansion mismatches. These mismatches induce high densities of threading dislocations, which act as non-radiative recombination centers that cause severe thermal quenching at elevated temperatures [6].

Achieving robust high-temperature performance is critical for the practical application of Si-based light sources. For example, lasers must exhibit high thermal stability against wavelength drift and efficiency drop to maintain sensing precision [7]. Quantum dot (QD) active regions are widely employed to improve the temperature stability of lasers due to their high defect tolerance [8]. Although InAs QD lasers on Si have demonstrated a characteristic temperature (T_0) exceeding 200 K at 1.3 µm [9], obtaining comparable stability in the NIR band remains challenging for InP-based QDs. Conventionally, AlGaInP has been used as the barrier material for InP QDs; however, the carrier confinement in this system is often restricted by a relatively small conduction band offset. Furthermore, atomic ordering in AlGaInP materials can reduce the effective bandgap and exacerbate thermal carrier escape [10,11]. Alternatively, the InP/GaAsP system eliminates such ordering-related limitations and has been adopted to demonstrate high-performance lasers on Si substrates [12]. Previous studies have shown that increasing the active-region stacking from 3 to 5 layers in InP/GaAsP QD lasers on Si can improve T_0 from 43 to 74 K [13]. Further improving the thermal performance on Si to approach the results on GaAs substrates is still required.

In this work, we demonstrate 780-nm InP/GaAsP QD lasers monolithically grown on (001) Si with an optimized 5-layer active region. A T_0 of 125 K was achieved in the 20–50 °C range, representing a significant improvement over the 75 K measured for the 3-layer reference samples on Si. The 5-layer lasers exhibit pulsed operation up to 95 °C with a low room-temperature (RT) threshold current density of 0.86 kA/cm^2 and a characteristic spectral shift of 0.25 nm/°C.

The InP/GaAsP QD laser structures were directly grown on GaAs and Si substrates by metal-organic chemical vapor deposition (MOCVD) in a single 4-inch system (AIXTRON 200/4). A schematic of the InP/GaAsP QD laser is shown in Fig. 1(a). The growth details for the GaAs on planar Si (GoPS) substrates have been previously reported [14]. The complete laser structure consists of several layers in order of growth: a 700-nm n-GaAs contact layer, an 800-nm n-$Al_{0.7}Ga_{0.3}As$ cladding layer, the active region, an 800-nm p-$Al_{0.7}Ga_{0.3}As$ cladding layer, and a 230-nm p-GaAs contact layer. These relatively thick cladding layers ensure sufficient optical mode confinement. Detailed doping concentrations for each layer are described in our previous work [13]. The active region is composed of InP QDs embedded in two 4-nm $GaAsP_{0.14}$ quantum wells (QWs), forming a dot-in-well (DWELL) structure sandwiched between two $Al_{0.4}Ga_{0.6}As$ barriers. To investigate the effect of active region stacking on modal gain enhancement, both 3-layer and 5-layer stacked QD structures were grown with each QD layer separated by a 20-nm $Al_{0.4}Ga_{0.6}As$ spacer. All layers were grown at 650 °C, except for the InP QDs, which were grown at 680 °C.

RT micro-photoluminescence (µ-PL) measurements were performed under 514-nm continuous-wave (CW) excitation with

Corrected 2 July 2026

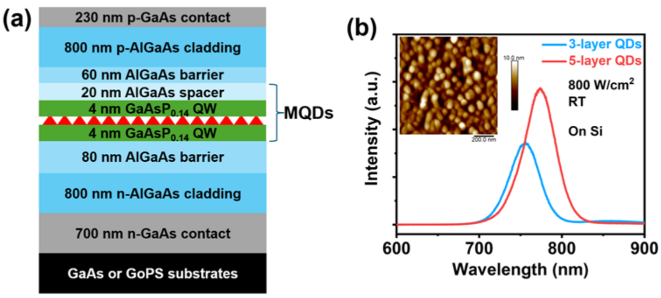

Fig. 1. (a) Schematic of the InP/GaAsP QD lasers grown on GaAs or Si substrates. (b) RT μ-PL spectra of the 3-layer and 5-layer QD structures grown on Si substrates. Inset: 1 × 1 μm^2 AFM image of uncapped 5-layer QDs grown on Si substrates.

a power density of 800 W/cm^2. As shown in Fig. 1(b), the 3-layer and 5-layer QD structures show primary emission peaks at 756 and 772 nm with measured full width at half maximum (FWHM) of 46 and 48 nm, respectively. The peak PL intensity of the 5-layer structure is around 1.7 times that of the 3-layer structure. This narrow FWHM and stronger PL intensity indicate high crystalline quality and size uniformity of QDs even after stacking more layers on Si. Surface morphology and QD density were evaluated by atomic force microscopy (AFM) on uncapped samples. As shown in the insert of Fig. 1(b), the QD density of the 5-layer structure on Si is approximately 1.8×10^{10} cm^{-2}. Notably, these QDs maintain high uniformity without significant coalescence even after stacking five layers. The 3-layer QDs on Si show similar AFM results (not shown here). In our previous work, a 5-layer QD structure grown on a $GaAsP_{0.40}$ matrix exhibited a small QD size and yielded a low laser T_0 on Si [13]. Although subsequently optimizing the QD size in a $GaAsP_{0.35}$ matrix, the multi-layer stack suffered from large, coalesced islands due to excessive strain, restricting the results to only GaAs platforms [15]. In this study, the phosphorus content is reduced to 0.14 in the GaAsP QWs compared to Ref. [15] to manage the accumulated strain and enable multi-stack growth.

The as-grown InP QD structures were fabricated into ridge waveguide lasers with cavity lengths ranging from 0.5 to 2 mm and ridge widths from 6 to 70 μm by standard photolithography, dry etching, and metallization [16]. To facilitate cleaving and improve thermal dissipation, the Si substrate was thinned down to 100–120 μm via mechanical lapping. Scanning electron microscope (SEM) inspection confirmed that the cleaved facets were smooth and mirror-like, providing good optical feedback (not shown here). These laser bars were characterized directly after cleaving without any facet coatings or specialized packaging. The 5-layer structure on Si serves as the primary device under investigation, while the 3-layer structure on Si and the 3-layer and 5-layer structures on GaAs with identical growth parameters and fabrication process serve as reference samples. During the measurement, these cleaved laser bars were placed on a temperature-controlled copper stage. To minimize Joule heating effects, these lasers were driven by a pulsed current source with a pulse width of 400 ns and a duty cycle of 0.5%. Figure 2(a) shows the representative current–voltage (*I–V*) characteristics of the 3-layer and 5-layer QD lasers on Si with a device dimension of 1.2 mm × 10 μm. Both devices exhibit a consistent turn-on voltage of around 1.5 V. Although the 5-layer QD laser shows a slightly higher on-resistance compared to the 3-layer QD laser (13 vs 9 Ω), both values remain sufficiently

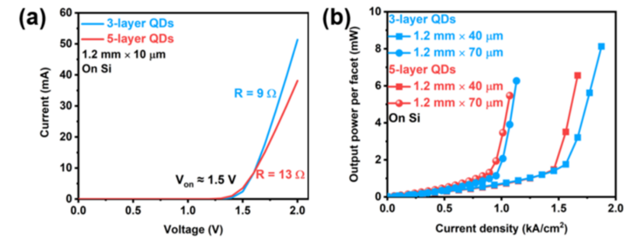

Fig. 2. (a) *I–V* characteristics of the 3-layer and 5-layer QD lasers on Si with a device dimension of 1.2 mm × 10 μm. (b) Representative *L–J* characteristics of the 3-layer and 5-layer QD lasers on Si.

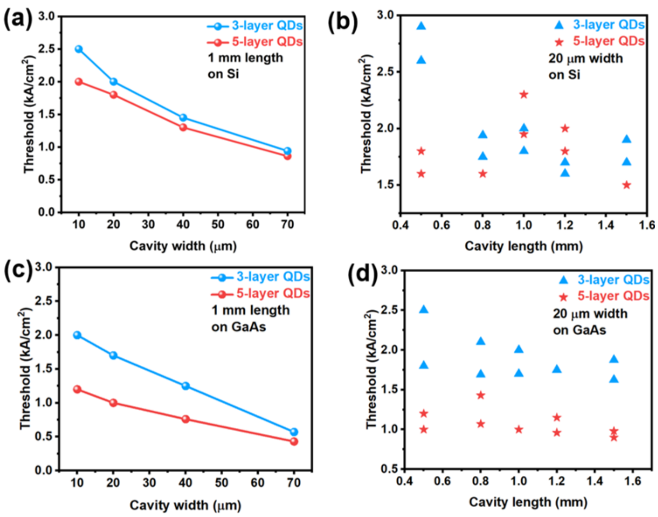

Fig. 3. (a) Cavity width and (b) cavity length dependence on threshold for the 3-layer and 5-layer QD lasers on Si substrates. (c) Cavity width and (d) cavity length dependence on threshold for lasers on GaAs substrates.

low, indicating the formation of good ohmic contact. Figure 2(b) shows the representative light-current density (*L-J*) characteristics of the 3-layer and 5-layer QD lasers on Si at RT. For a device dimension of 1.2 mm × 70 μm, threshold current densities (J_{th}) of 0.94 and 0.86 kA/cm^2 were obtained for the 3-layer and 5-layer QD lasers, respectively.

To investigate the effect of active-region stacking on J_{th}, Figs. 3(a)–3(d) compare the J_{th} evolution with increasing device dimensions for the 3-layer and 5-layer devices on Si and GaAs substrates. The 5-layer devices exhibit lower J_{th} across most of the measured ridge widths and lengths on both substrates, except for some experimental variations for 1- and 1.2-mm cavity lengths on Si. Based on the J_{th} condition [17], when the cavity length is very short (e.g., 0.5 mm), the mirror loss increases significantly, and the mode gain is negatively correlated with J_{th}. Therefore, the reduced J_{th} for 5-layer devices is due to the increase in their mode gain. In addition, 5-layer devices allow the threshold condition to be met at a lower carrier occupancy per dot [18]. Consequently, this minimizes heat generation and suppresses carrier thermal escape into the barrier layers, enhancing thermal stability. It is worth noting that while further increasing the number of QD layers could potentially enhance the gain, adding too many layers may lead to excessive strain and the degradation of material quality.

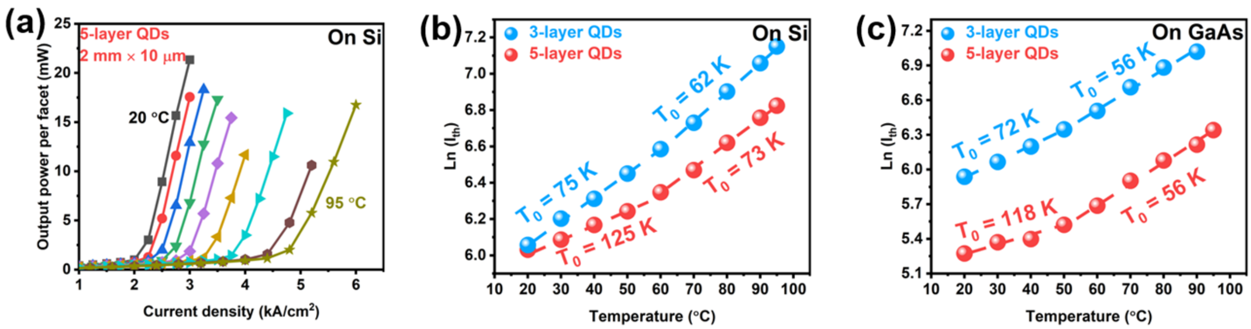

Fig. 4. (a) Temperature-dependent *L–J* characteristics from 20°C to 95°C for the 5-layer QD laser on Si (2 mm × 10 μm). Comparison of extracted T_0 of 3-layer and 5-layer QD lasers on (b) Si and (c) GaAs substrates.

Table 1. Comparison of T_0 for MOCVD-Grown InP QD Lasers

Ref.	Wavelength (nm)	Stacking Number	T_0 (K)	Substrate
[13]	757	5	74 K (20–95 °C)	Si
[15]	755	1	55 K (20–60 °C), 30 K (60–95 °C)	GaAs
[22]	638	1	124 K (5–20 °C), 49 K (20–40 °C)	GaAs
[23]	660	1	85 K (5–25 °C), 53 K (5–55 °C)	GaAs
[24]	741	5	52 K (10–85 °C)	GaAs
[25]	774	5	111 K (7–47 °C), 89 K (47–87 °C)	GaAs
This work	**752**	**3**	**72 K (20–50 °C), 56 K (50–90 °C)**	**GaAs**
	771	**5**	**118 K (20–50 °C), 56 K (50–90 °C)**	**GaAs**
	765	**3**	**75 K (20–50 °C), 62 K (50–95 °C)**	**Si**
	780	**5**	**125 K (20–50 °C), 73 K (50–95 °C)**	**Si**

To evaluate the thermal stability, the temperature-dependent *L–J* characteristics of the 5-layer QD laser on Si were measured from 20 to 95 °C, as shown in Fig. 4(a). The device demonstrates robust pulsed operation up to 95 °C, with the *L–J* curves maintaining a clear threshold behavior throughout the entire temperature range. To quantify the thermal robustness, the T_0 values were extracted by fitting the threshold current density using the empirical formula $J_{th} = J_0\, exp(T/T_0)$ [19]. Figures 4(b) and 4(c) show the comparative T_0 analysis for both 3-layer and 5-layer QD lasers on Si and GaAs substrates, respectively, with the devices on GaAs fabricated identically along with Si providing a baseline. For the 5-layer QD laser on Si, a high T_0 of 125 K was achieved in the 20–50 °C range, representing a significant improvement over the 75 K measured for the 3-layer counterpart on Si. Above 50 °C, both devices exhibit a typical reduction in T_0 due to increased thermal carrier escape [20,21]; however, the 5-layer QD laser on Si maintains a higher T_0 of 73 K, outperforming the 62 K of the 3-layer QD laser on Si. A consistent trend of enhanced thermal stability through active-region stacking is also observed on GaAs substrates [Fig. 4(c)]. The superior T_0 in the 5-layer QD laser is primarily attributed to the increased modal gain provided by the additional QD layers. Besides, these T_0 values for the device on Si are higher than those on GaAs, which is attributed to the higher thermal conductivity of Si [13].

Table 1 presents a comparative study of T_0 between our work and other reported MOCVD-grown InP QD lasers operating in the 630–800 nm range. The optimized 5-layer device on Si demonstrates superior thermal stability with a high T_0 value at 780 nm, which is highly competitive with those of lasers. These findings confirm that increasing the stacking layers of the active region significantly enhances thermal stability and provides a robust solution for high-T_0 light sources directly onto Si platforms.

Figure 5(a) shows the temperature-dependent lasing spectra of the 5-layer QD laser on Si, measured from 20 to 90 °C at $1.2 J_{th}$. The device maintains multimode lasing across the entire temperature range. The intensity-weighted centroid wavelengths across the entire continuous spectral profile were extracted from the spectra at each temperature to avoid mode-hopping errors [26], and the results are plotted in Figs. 5(b) and 5(c). As the temperature increases, the lasing peaks exhibit a clear redshift. For the 5-layer QD laser on Si and GaAs, wavelength tuning rates of 0.25 and 0.28 nm/°C are obtained by linear fitting. Meanwhile, the 3-layer QD lasers on both Si and GaAs show a similar tuning rate of 0.25–0.26 nm/°C. These values align with the typical range of 0.25–0.35 nm/°C reported for 780 nm lasers [27]. The linear redshift of the lasing wavelength is primarily governed by the temperature-induced bandgap shrinkage of the active region. The similar thermal tuning behavior between the 5-layer QD laser on Si and GaAs exhibits the high material quality of our monolithically integrated Si-based light sources.

In summary, we have demonstrated 780-nm InP/GaAsP QD lasers monolithically grown on (001) Si substrates. By employing the active region with a 5-layer QD stack, the thermal stability of the devices was markedly improved. A T_0 value of 125 K was achieved in the 20–50 °C range, representing a significant increase over the 75 K measured for the 3-layer QD counterpart on Si. The devices sustained pulsed operation up to 95 °C with a wavelength tuning rate of 0.25 nm/°C, which aligns with the performance of devices on GaAs substrates. These results indicate that optimized active-region stacking is an

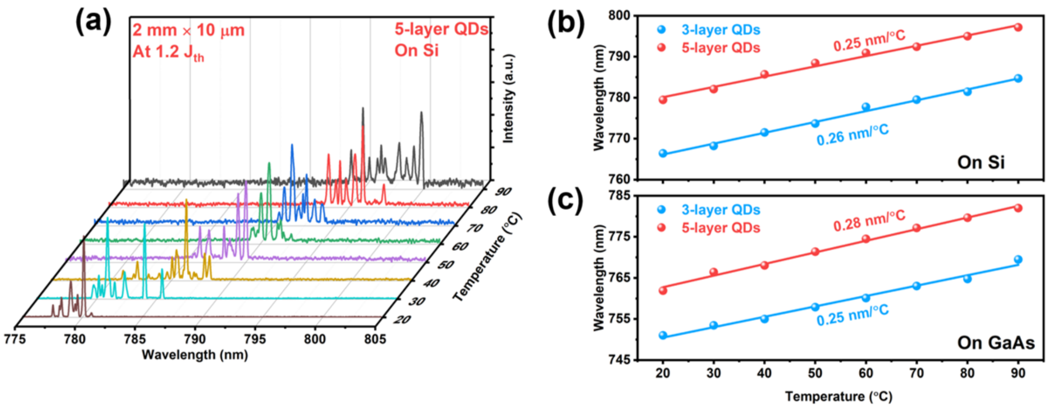

Fig. 5. (a) Temperature-dependent lasing spectra of the 5-layer QD lasers with a device dimension of 2 mm × 10 μm at 1.2 times threshold current. Temperature-dependent lasing peaks of 3-layer and 5-layer QD lasers on (b) Si and (c) GaAs substrates.

effective approach to mitigate the thermal bottleneck of InP QD NIR lasers on Si platforms.

Funding. Innovation and Technology Fund (ITS/201/19FP).

Acknowledgment. The authors would like to thank Nanosystem Fabrication Facility (NFF) and the Material Characterization Preparation Facility (MCPF) of HKUST for their technical support.

Disclosures. The authors declare no conflicts of interest.

Data availability. Data underlying the results presented in this paper are not publicly available at this time but may be obtained from the authors upon reasonable request.

REFERENCES

1. D. Liang and J. E. Bowers, Nat. Photonics **4**, 511 (2010).
2. S. Shekhar, W. Bogaerts, L. Chrostowski, *et al.*, Nat. Commun. **15**, 751 (2024).
3. J. Wang, F. Sciarrino, A. Laing, *et al.*, Nat. Photonics **14**, 273 (2020).
4. A. Müller, S. Marschall, O. B. Jensen, *et al.*, Laser Photonics Rev. **7**, 605 (2013).
5. M. Hardy and H. O. M. Chu, Analyst **150**, 1986 (2025).
6. J. Selvidge, J. Norman, M. E. Salmon, *et al.*, Appl. Phys. Lett. **115**, 131102 (2019).
7. M. Nourhashemi, M. Mahmoudzadeh, and F. Wallois, Neurophotonics **3**, 015001 (2016).
8. S. Chen, W. Li, J. Wu, *et al.*, Nat. Photon. **10**, 307 (2016).
9. Z. Lv, S. Wang, S. Wang, *et al.*, Opt. Express **31**, 24173 (2023).
10. T. Suzuki, A. Gomyo, S. Iijima, *et al.*, Jpn. J. Appl. Phys. **27**, 2098 (1988).
11. A. Moritz and A. Hangleiter, Appl. Phys. Lett. **66**, 3340 (1995).
12. W. Luo, Q. Lin, J. Huang, *et al.*, in 28th International Semiconductor Laser Conference (ISLC), (2022), p. **1**.
13. W. Luo, L. Lin, J. Huang, *et al.*, Opt. Express **30**, 40750 (2022).
14. J. Huang, Q. Lin, W. Luo, *et al.*, J. Appl. Phys. **132**, 193103 (2022).
15. W. Gu, S. Lamon, M. Gu, *et al.*, Opt. Express **33**, 16317 (2025).
16. Y. Xue, W. Luo, S. Zhu, *et al.*, Opt. Express **28**, 18172 (2020).
17. Q. Lin, J. Huang, L. Lin, *et al.*, Opt. Express **31**, 15326 (2023).
18. D. Zhou, R. Piron, M. Dontabactouny, *et al.*, Phys. Status Solidi C **6**, 2217 (2009).
19. A. Y. Liu, C. Zhang, J. Norman, *et al.*, Appl. Phys. Lett. **104**, 041104 (2014).
20. L. V. Asryan and R. A. Suris, IEEE J. Quantum Electron. **34**, 841 (1998).
21. H. Y. Liu, D. T. Childs, T. J. Badcock, *et al.*, IEEE Photonics Technol. Lett. **17**, 1139 (2005).
22. W. M. Schulz, M. Eichfelder, R. Roßbach, *et al.*, Appl. Phys. Express **2**, 112501 (2009).
23. Z. Huang, M. Zimmer, S. Hepp, *et al.*, IEEE J. Quantum Electron. **55**, 1 (2019).
24. A. B. Krysa, S. L. Liew, J. C. Lin, *et al.*, J. Cryst. Growth **298**, 663 (2007).
25. M. S. Al-Ghamdi, N. A. Al-Anazi, and I. B. Karomi, Res. Opt. **21**, 100835 (2025).
26. K. Hieda, T. Maruyama, T. Takesako, *et al.*, Opt. Rev. **25**, 175 (2018).
27. L. Zhu, W. Liu, J. Qin, *et al.*, IEEE Photonics J. **17**, 150016 (2024).